Serum proteomics analysis reveals the thermal fitness of dairy buffalo to chronic heat stress

Liu Ping
Yunnan Agricultural University
Guo Lulu
Yunnan Agricultural University
Mao Huaming
Yunnan Agricultural University
Gu Zhaobing (zhaobinggu@163.com)
Yunnan Agricultural University https://orcid.org/0000-0001-6175-623X

Research article

Keywords: Thermal fitness, Chronic heat stress, Dairy buffaloes, Proteomics

Posted Date: August 20th, 2019

DOI: https://doi.org/10.21203/rs.2.13215/v1

Abstract

Background: Chronic heat stress (CHS), aggravated by global warming, reduces the production efficiency of the buffalo dairy industry. CHS changes protein abundance, and low-abundant proteins take important roles in biological processes. Results: The objective of the study was to assess differences in low-abundant serum proteins in dairy buffaloes at thermoneutral (TN) or under chronic heat stress (CHS) conditions with proteomic approaches. Six dairy buffaloes as reference animal raised in TN season, and another six dairy buffaloes raised in CHS to discover the molecular mechanism of thermal fitness in hot season with serum proteomics. After the removal of multiple high-abundant proteins in serum, 344 low-abundant proteins were identified in serum with label-free quantification. Of these, 17 low-abundant differentially expressed serum proteins with known functions were detected, and five of these differentially expressed proteins were validated with parallel reaction monitoring. These five proteins were associated with various aspects of heat stress, including decreased heat production, increased blood oxygen delivery, and enhanced natural disease resistance. Conclusions: Lipase (LPL), glutathione peroxidase 3 (GPX3), cathelicidin-2 (CATHL2), ceruloplasmin (CP), and hemoglobin subunit alpha 1 (HBA1) were shown to play cooperative roles in CHS fitness in dairy buffalo. Dairy buffaloes adapt to CHS and hypoxia with high levels of RBCs, HBA1 and CP increased blood oxygen delivery capacity and thermal fitness.

Background

In 2016, global population of domestic buffalo (*Bubalus bubalis)* was ~199.0 million; about 99% of buffalo inhabit tropical and subtropical regions. At present, the mean daily maximum temperature across the regions where buffalo are raised is 19.7–41.2 ºC, but it is predicted that the daily maximum temperature in these regions will increase by 1–4.5 ºC over the next 50 years. Although buffalo are well adapted to hot climates, they show signs of thermal discomfort, such as low milk yield and poor reproductive performance, at temperatures exceeding 25ºC. At ambient temperatures of 29.4°C and 38.9°C, nutrient intake and milk yield decreased ~30.0% and ~27.6% for dairy cattle, respectively [1]. In addition, buffalo have fewer sweat glands than do cattle, increasing heat sensitivity [2]. Thus, buffaloes are particularly sensitive to heat stress (HS) as global warming progresses, threatening the buffalo dairy industry [3, 4].

Chronic heat stress (CHS) occurs after prolonged exposure to elevated ambient temperatures and high humidity, when the animal is unable to dissipate excessive heat load to the surrounding environment [5]. CHS stimulates the excessive accumulation of reactive oxygen species (ROS), which triggers the oxidative stress response [6]. High concentrations of ROS limit energy production and utilization in heat-stressed animals [7], negatively affecting animal growth, production, and reproductive performance. To improve the production efficiency of dairy buffalo, it is important to investigate the mechanisms underlying CHS thermal fitness using protein biomarkers.

Proteomics have been widely used to assess the ability of livestock to adapt to temperature increases [8]. Specifically, label-free quantification (LFQ) is a high-resolution method based on mass spectrometry, which determines the relative amounts of protein among two or more biological samples without the use of stable isotopes). LFQ extracts peptide signals on the MS1 level, and thus uncouples the quantification process from the identification process. Single and multiple reaction monitoring (SRM/MRM) methods have been widely used for protein absolute quantification due to their high sensitivity, accuracy, and repeatability. Parallel reaction monitoring (PRM) is an ion monitoring technique (5–6 orders of magnitude), which detects all product ions in parallel in a high-precision mass spectrometer [9]. The principle of this technique is similar to SRM/MRM, but PRM is more convenient and selective than SRM/MRM [10]. PRM is thus the most suitable for the quantification of multiple proteins with an attomole-level of detection.

For livestock, blood sampling is convenient, and blood biomarkers are useful indicator of the physiological state of the animal [11]. Because low-abundant proteins (transcripts) may play important roles in biological processes [12], we thus analyzed low-abundant serum proteins from dairy buffaloes under CHS and thermoneutral (TN) conditions with proteomics approaches. Low-abundant serum proteins were detected with LFQ, and the differential abundant proteins were validated with PRM. In this way, we aimed to identify protein biomarkers to increase our understanding of the CHS fitness in dairy buffalo.

Methods

Experimental location

The experiment was carried out at a dairy buffalo farm, Dehong state, China which is located in the hot and humid climate zone at longitude 98.57ºE and latitude 24.43ºN and at an altitude of 870 m above mean sea level. Temperature-humidity index (THI) is widely used to evaluate the degree of heat stress for dairy animal. Temperature and humidity loggers (±0.2°C; Testo 175H1), placed 2.0 m above the floor of the bedding area, recorded ambient temperature and relative humidity at 30 min intervals to calculate THI with the following formula [13]:

$$THI = (1.8 \times T + 32) - (0.55 - 0.0055 \times RH) \times (1.8 \times T - 26),$$

T - Ambient temperature (°C), RH - Relative humidity (%)

Average THI was ≥72 in summer based on meteorological data from 2005 to 2015. Also, THI is not exceed 60 in winter in recent decades and even during the field trail. It is sure that dairy buffaloes adapt to the comfortable climate.

Experimental animals and management

In hot summer (average THI 75.76), 6 multiparous (parity = 3) Nili-Ravi × Murrah × local crossbred female buffaloes in mid-lactation were used for the CHS experiment (CHS group) at this site between July 20 and August 4, 2016. Under thermoneutral conditions, 6 multiparous dairy buffaloes (parity = 3) in mid-lactation were selected as the reference animals (TN group) between January 3 and January 18, 2017 (average THI 54.26). All animals were loose housed, and provided with fresh drinking water ad libitum. Animals were fed the same mixed rations (80% whole-plant corn silage ad libitum, 12.5% feed concentrate, and 7.5% corn protein powder) in the CHS and TN field trails. The nutritional value of the three feed ingredients is shown in Table S1.

Respiration rates were counted with a stopwatch at 08:00, 13:00 and 18:00 h, when dairy buffalo were quiet. The chest movements in a continuous 3 min were converted to breaths min^{-1}, and each measurement was recorded three times to obtain average value. A waterproof micro-temperature sensor (±0.5°C; DS1922L, Wdsen Electronic Technology Co., Ltd), fixed in the slot of a T-shaped controlled internal drug release device (without progesterone; DEC International NZ Ltd), was placed in the vagina of each buffalo. This device recorded body temperature at 30 min intervals.

Removal of High-abundant Serum Proteins

At the end of the field trail (15 d), blood samples were collected with vacutainer tubes via jugular venipuncture. Each sample was centrifuged at 1,400 × g for 10 min to separate the serum. Serum samples were stored at –80°C. Affinity chromatographic columns (Agilent Multiple Affinity Removal LC Columns) was performed to remove high-abundant serum proteins in serum samples. Low-abundant serum proteins were isolated by first performing an ultrafiltration concentration, then adding one double volume of SDT buffer (4% SDS, 100 mM Tris-HCl, and 1 mM DTT; pH 7.6) to the concentrated sample. The resultant mixture was then incubated in a boiling water bath for 15 min. The mixture was then centrifuged at 14,000 × g for 20 min, and the supernatant was transferred to a clean tube. We then added 20 μg of the supernatant to 5 × loading buffer (10% SDS, 0.5% bromophenol blue, 50% glycerol, 500 mM DTT, and 250 mM Tris-HCl; pH 6.8). This mixture was incubated in a 90°C water bath for 5 min, and then analyzed using 12.5% SDS-PAGE (constant 14 mA current for 90 min) with Coomassie blue staining.

Protein Digestion with Filter-aided Sample Preparation Protocols

Trypsin protein digestion was performed using the filter-aided sample preparation protocols described previously [14]. In brief, serum samples were lysed, and proteins were extracted using SDT buffer. Proteins were quantified with BCA Protein Assay Kits (Bio-Rad). We then analyzed 20 μg of each extracted protein sample with SDS-PAGE. Next, 100 μg of extracted protein was dissolved in DTT (to generate a final concentration of 10 mM) in a 90°C water bath for 15 min, and then cooled to room temperature. Small molecules and detergent were extracted using 10 kD ultrafiltration with 200 μL UA buffer (8 M Urea and 150 mM Tris-HCl; pH 8.0). The mixture was centrifuged for 120 min (14,000 × g) to discard the filtrate. We then added 100 IAA buffer (50 mM IAA in UA buffer) to the concentrate. Prior to centrifugation, this mixture was shaken at 600 rpm for 1 min, and then incubated for 30 min in the dark.

After incubation, the mixture was centrifuged at 14,000 × g for 20 min. The filter was washed three times with 100 μL of UA buffer and centrifuged at 14,000 × g for 20 min. Then, the filter was washed twice with 100 μL of 50 mM NH_4HCO_3 buffer. Finally, the protein suspension was added to 40 μL of NH_4HCO_3 buffer (2 μg Lys-C) and incubated in a 37°C water bath for 4 h. We added 2 μg trypsin to the protein mixture, and then incubated the mixture in a 37°C water bath for 16 h. After incubation, the protein mixture was transferred to a fresh reaction tube, and centrifuged at 14,000 × g for 15 min. Finally, the filter was washed with 40 μL of 50 mM NH_4HCO_3 buffer, and centrifuged at 14,000 × g for 30 min. The filtrate was collected and desalinated with a C18 Cartridge (Empore SPE Cartridges C18 [standard density], Sigma; bed inner diameter 7 mm; volume 3 ml). Desalted samples were freeze-dried, and peptide levels were determined at OD280. Peptide samples were then stored at −80°C until the time of further studies.

LFQ with LC-MS/MS Analysis

LFQ experiment was conducted at Shanghai Applied Protein Technology Co. Ltd in China. LC-MS/MS was performed using a Q-Ex active mass spectrometer (Thermo Scientific) coupled to an Easy nLC 1200 (Proxeon Biosystems, now Thermo Fisher Scientific) with an analysis time of 60 min. First, peptides were loaded onto a reverse phase trap column (Thermo Scientific Acclaim PepMap100; 100 μm × 2 cm; nanoViper C18) connected to a C18-reversed phase analytical column (Thermo Scientific Easy Column; 10 cm long, 75 μm inner diameter, 3 μm resin) in buffer A (0.1% formic acid). Peptides were separated using a linear gradient of buffer B (84% acetonitrile and 0.1% formic acid) at a flow rate of 300 nl/min, controlled by an IntelliFlow technology. The linear gradient in the trap column was as follows: 0–35% solution B from 0–50min; 35–100% solution B from 50–55min; 40–100% solution B from 55–60min; and hold at 100% solution B.

MS raw data were combined and searched using MaxQuant 1.3.0.5 software [15], which uses the Andromeda search engine against the Bovinae Uniprot database. The precursor mass tolerance was set to 20 ppm for the first Andromeda search, and to 6 ppm for the main search. Carbamidomethylation (C) was considered a fixed modification, while oxidation (M) and acetylation (of the protein N-terminus) were considered variable modifications. We eliminated all peptide and protein identifications where the false discovery rate (FDR) was >0.01 against the reversed-sequence database.

We used MaxQuant 1.3.0.5 software to perform identifications of proteins and LFQ, enabling ‘match between runs’ with a retention time window of 2 min, and setting the LFQ minimum ratio count to 1. Using the relative abundance of proteins in TN buffalo as a reference, we identified CHS-buffalo proteins as significantly differentially expressed if these proteins were identified in at least two of three replicates with a fold change >1.5 (< 0.67) and a p <0.05. We used volcano plots to visualize the differentially expressed proteins. We then performed a hierarchical clustering analysis of the low-abundant differentially expressed serum proteins between the CHS and TN buffalo using the $\log_2$-transformed expression values and a cutoff of $p < 0.05$.

Quantification of Targeted Proteins with PRM

The PRM was conducted at Shanghai Applied Protein Technology Co. Ltd in China. The Easy nLC 1200 (Thermo Scientific) was used for chromatographic separation. First, peptides were separated with a binary solvent system consisting of 0.1% formic acid (solvent A) and 0.1% formic acid acetonitrile (84% acetonitrile) (solvent B). We used 95% solvent A as the equilibrium liquid for the analytical column (Thermo Scientific EASY column). We added 20 fmol of a standard peptide to 2 μg of the separated peptides. The peptide mixture was then separated at a flow rate of 250 nl/min, with a linear gradient in the trap column (5–23% solution B from 0–42 min; 23–40% solution B from 42–50 min; 40–100% solution B from 50–60 min; and hold at 100% solution B).

We selected proteins for PRM validation that were significantly more abundant and closely associated with CHS fitness. We examined the peptides eluted by the nano-high-performance LC using PRM positive ion mass spectrometry on a Q-Ex active HF mass spectrometer system (Thermo Scientific). MS spectra were acquired in the m/z range 300–1800, with an *R* of 60,000 at m/z 200. Automatic gain control (AGC) was set to 3e6, with a max injection time of 200 ms. We then selected 20 PRM/MS2 scans for higher-energy collisional dissociation experiments that conformed to the following parameters: 1.6 Th isolation window; *R* of 30,000 at m/z 200; 3e6 AGC; 120 ms maximum injection time; MS2 higher-energy collisionally activated dissociation (HCD); and a normalized collision energy of 27.

We analyzed the PRM raw data from the 12 CHS and TN samples with Skyline v3.5.0 [16]. The peptide settings used for the Skyline import were consistent with the MaxQuant search parameters (i.e., enzyme set to trypsin; max missed cleavages set to 2). Two or three consecutive high-intensity peptides were selected for import into Skyline to determine the number of targeted proteins, the sequences of the targeted peptides, the charges of the parent ions, and the peak areas. Total peak areas were calibrated against internal standard peptides, heavy isotopes [17]. Based on these total peak areas, we quantified each target peptide.

Bioinformatics Analysis

We identified protein sequences homologous to those of the selected differentially expressed proteins with the NCBI BLAST+ client (ncbi-blast–2.2.28+-win32.exe) and InterProScan) [18]. We then annotated protein sequences using gene ontology (GO) terms with Blast2GO. The GO annotation results were plotted with R scripts. Following annotation, the differentially expressed protein sequences were blasted against the Kyoto Encyclopedia of Genes and Genomes (KEGG) database (http://geneontology.org/) to identify KEGG Orthology. Differentially expressed proteins were subsequently mapped to KEGG pathways.

A functional protein interaction network for our differentially expressed proteins was constructed using STRING (https://string-db.org/), searching by multiple protein names. As few protein–protein interactions (PPI) are yet available in the *Bos taurus* STRING database, we searched for these interactions in the *Homo sapiens* database.

Hematological parameters

We measured hemoglobin level (Hb), red blood cell count (RBC), white blood cell count (WBC), hematocrit (HCT), mean corpuscular hemoglobin concentration (MCHC), mean corpuscular hemoglobin (MCH), platelet hematocrit (PLT), and mean corpuscular volume (MCV) in the whole blood samples using a fully automated biochemical analyzer (Sysmex XT–1800i) within 24 h of blood collection.

Results

Physiological parameters of buffaloes under CHS or TN Conditions

Climate conditions (air temperature and THI) and respiratory rates of dairy buffaloes were shown in Fig 1. The average air temperature is 25.7°C and 12.8°C under the CHS and TN conditions, respectively ($p < 0.001$). The average THI values were 75.8 and 54.3 under the CHS and TN conditions, respectively ($p < 0.001$). Body temperatures of the CHS and TN buffalo averaged across the whole duration of the trial were 38.6°C and 38.3°C, respectively ($p > 0.05$). Respiratory rates of the CHS buffalo were significantly greater than that of the TN buffalo ($p < 0.001$).

Identification of proteins related to CHS fitness

Using LFQ, 344 low-abundant serum proteins were identified in serum samples. Of these, our LFQ results indicated that 17 were differentially expressed in CHS buffalo as compared to the TN buffalo (Table 1). Volcano plot indicated that four of these proteins were more abundant in CHS buffalo, while 13 were less abundant (Fig. 2). Hierarchical clustering analysis indicated that the 17 differentially abundant proteins grouped well by function: proteins similar to resistin (RETN) formed one cluster, and the other cluster comprised ceruloplasmin (CP: L8I5R0 and D2U6Z5), hemoglobin subunit alpha1 (HBA1), and cathelicidin–2 (CATHL2, LL–37). L8I5R0 and D2U6Z5, both representing CP, were obviously closely clustered (Fig. 3).

Interestingly, four of the differentially abundant proteins identified by both LFQ and PRM were enzymes. Of these, CP (L8I5R0, D2U6Z5 [EC:1.16.3.1]), HBA1 (Q9TSN7) and LL–37 (A0A0A7V3V9) were significantly more abundant in CHS buffalo as compared to TN buffalo ($p < 0.05$ for all): HBA1 (3.76-fold increase), CP (1.50-fold increase) and LL–37 (1.84-fold increase) (Fig. 4). The remaining enzymes, lipoprotein lipase (LPL-[EC:3.1.1.34]) and glutathione peroxidase 3 (GPX3, [EC:1.11.1.9]), were significantly less abundant in CHS buffalo as compared to TN buffalo (0.59-fold and 0.35-fold decrease, respectively; $p < 0.05$; Table 1).

Gene ontology analysis, and protein-protein interaction.

We identified GO terms that were highly enriched in the 17 differentially expressed proteins identified by LFQ (Tables 2 and 3). One set of enriched GO terms was associated with associated with redox reactions (GO:0003824, GO:0016491), lipase activity (GO:0006629), hydrolysis (GO:0016787), which increase the

ability of response to stress (GO:0006950). A second set was associated with correct protein folding or the degradation of mis-folded proteins (GO: 0031625). The third set of enriched GO terms were associated with regulation of blood circulation (GO:1903522), oxygen binding and delivery (GO: 0019825).

In parallel studies, we analyzed the correlations among the 17 differentially abundant proteins identified by LFQ, and quantified the metabolites [19]. Four proteins were mapped to KEGG metabolic pathways: GPX3, CP, CD14, and LL–37. GPX3 and CP produce glutamic acid; similar amounts of glutamic acid were produced by the CHS buffalo (34.2 μM) and the TN buffalo (26.8 μM; $p > 0.05$). CD14 and LL–37 produce acetylcholine; significantly more acetylcholine was produced by the CHS buffalo (0.19 nM) than the TN buffalo (0.16 nM; $p < 0.001$). GPX3 was associated with the glutathione metabolism pathway; CP was associated with the porphyrin metabolism pathway; CD14 was associated with the regulation of the actin cytoskeleton; and LL–37 was associated with salivary secretions.

Because both L8I5R0 and D2U6Z5 represent CP, We analyzed the PPI networks of 16 of the 17 differentially abundant proteins identified by LFQ. Monocyte differentiation antigen, carboxypeptidase N-catalytic chain precursor, hemoglobin subunit alpha1, hepatitis A virus cellular receptor 1 N-terminal domain containing protein, glycosylation-dependent cell adhesion molecule 1, thrombospondin–4 and phospholipase A1 member A were not included in the network (Fig. 5). This network had eight edges, with an average node degree of 1, and an average local clustering coefficient of 0.479. The expected number of edges was 2, giving a network enrichment *p*-value of 0.000221. In particular, two of the PPIs (lipoprotein lipase and resistin; ceruloplasmin and glutathione peroxidase 3) function synergistically to increase CHS fitness for buffalo.

Validation of LFQ results with PRM

We used PRM to validate the differential abundance of five proteins: CP (L8I5R0 and D2U6Z5), HBA1, LPL, LL–37, and GPX3 (Table 1). Three of these proteins (HBA1, CP, and LL–37) were identified as significantly more abundant in CHS buffalo as compared to TN buffalo by both LFQ and PRM (Fig. 4).

Hematological parameters

CHS buffalo had significantly lower levels of MCHC ($p < 0.05$) and MCH ($p < 0.01$) than did TN buffalo, and significantly higher levels of HCT and MCV ($p < 0.01$; Fig. 6). CHS buffalo had slightly higher levels of RBC, Hb and PLT, as well as slightly lower levels of WBC, but these differences were not significant.

Discussion

Seventeen proteins were differentially abundant in CHS buffalo as compared to TN buffalo. Several of these proteins were associated with functions related to HS. For example, HBA1, which was significantly more abundant in CHS buffalo, is involved in heme and iron binding, and transports oxygen from the

lungs to various inner organs and peripheral tissues. CP, playing important roles in iron delivery and protects cellular lipids from iron-dependent lipid peroxidation [20], was significantly more abundant in CHS buffalo.

Under normal condition, ROS (e.g., H_2O_2 and $O_2^{\bullet -}$) play important roles as signal molecules. However, HS triggers excessive ROS accumulation, causing damage to biological macromolecules. As a well-known redox protein and antioxidant enzyme, GPX3 protects cells from oxidative stress by decomposing H_2O_2 [21]. LFQ abundance analysis indicated that CHS buffalo had significantly lower levels of serum GPX3 than did TN buffalo, suggesting that the buffalo were experiencing CHS [22]. Consistent with this result, previous researches reported that farm animals (e.g., finishing broilers, cattle, and dairy cows) decreased GPX3 activity under HS conditions [23, 24, 25]. PRM analysis indicated that mean GPX3 levels in CHS buffalo were lower than those in TN buffalo. This suggested that CHS buffalo maintain normal GPX3 levels to protect cell membranes from oxidative damage. In addition, H_2O_2 inhibits protein refolding and leads to protein denaturation, which is detrimental to cellular structure and function [26]. Several GO terms significantly enriched in the differentially abundant proteins are known to promote correct protein folding and degrade mis-folded proteins (i.e., ubiquitin protein ligase binding, heat shock protein binding, and unfolded protein binding). This might imply that buffalo use posttranslational protein processing to handle CHS.

CHS impairs immune function in animals, and also increases susceptibility to infection [27]. LL–37, a small cationic antimicrobial peptide produced in the epithelial cells, disrupts the activity of gram-negative bacteria by damaging and destroying bacterial membranes [28]. LL–37 plays key roles in inflammatory response regulation and immune mediator induction [29]. In heat-stressed mice, LL–37 production was suppressed by the nicotinic acetylcholine system, increasing the susceptibility of the mice *Staphylococcus aureus* [30]. In CHS buffalo, LL–37 was significantly more abundant than in TN buffalo (based on both LFQ and PRM), suggesting that the CHS buffalo might increase the thermotolerance to infection. As LL–37 is important for the immune and inflammatory response [31], it is possible that the higher LL–37 serum levels seen here in CHS buffalo increase the defense against microbial invasions, compensating for the relatively low level of antioxidant enzymes (GPX3).

The low-abundant differentially serum proteins in CHS buffalo as compared to the TN buffalo were also significantly enriched in the GO term nitric-oxide synthase regulator activity, which is associated with peripheral vasodilatation [32]. In vasodilation, blood flow to the body surface is increased to enhance heat dissipation, and oxygen delivery to internal organs is improved. This was consistent with the high levels of HBA1 and RBC detected in the CHS buffalo.

We successfully mapped four proteins (GPX3, CP, CD14 and LL–37) and their corresponding metabolites to metabolic pathways. As a major neurotransmitter, acetylcholine participates in homoeothermic thermoregulation. Acetylcholine is also known to regulate glutamic acid release, and glutamic acid generates glutamate via pyroglutamic acid. Glutamate and GPX produce glutathione via the glutathione metabolism pathway [33], and GPX3 and glutathione protect the cell from heat injury [34]. Glutamic acid,

along with CP, is also involved in the porphyrin metabolism pathway, which increases HBA1 levels to improve oxygen delivery in HS animals. LL–37 and acetylcholine were mapped to the salivary secretion pathway. As buffalo, which have few sweat glands, dissipate only 12% of their excess heat through skin evaporation; salivary secretions help decrease body temperature [35].

Under HS conditions, high levels of hemoglobin lead to increased oxygen delivery [36]. PPI networks provide collaborative working modes for physiological and biological processes at the system-level [37]. We found that most of the 17 differentially abundant proteins in CHS buffalo as compared to TN buffalo were linked in the *H. sapiens* database (Fig. 5). CD14, CHST4, HBA1, SPARCL1, CPN1, THBS4, SPARCL1, and PLA1A were not linked to each other.

Hb and CP play a collaborative role in oxygen delivery, as CP oxidizes Fe^{2+} to Fe^{3+} without releasing ROS. We observed a concomitant increase in Hb and CP in CHS buffalo, consistent with a previous study [38]. However, to date, no biological interaction networks have shown a direct relationship between these proteins. These proteins were not linked in the PPI network, but Hb and CP are functionally similar, and their serum levels increased simultaneously. Previous studies have reported that RETN and LPL are important for glucose and lipoprotein metabolism [39], and the PPI between RETN and LPL indicated that the metabolic profiles of glucose and lipoprotein were altered by HS. Moreover, antioxidant enzymes GPX3 and non-enzymatic antioxidant CP protect cell from oxidative stress damage.

Under HS, homoeothermic animals facilitate heat dissipation by increasing body temperature, respiratory rates, and blood flow to the peripheral tissues [40]. The demands on the cardiovascular system also increase with HS, as does arterial blood pressure, causing internal tissues and organs to compete with peripheral areas for blood supply [41]. Eventually, low blood flow volume may result in the hypoxia of the internal organs and inflammation [42, 43]. Body temperature and blood flow are closely associated [44]: it was shown that blood flow to internal organs decreased 20–40% in heat-stressed rabbits.

HS cattle decreased ~12–20% RBCs as compared to TN cattle [45]. Here, the RBC of the CHS buffalo was not significantly different from that of the TN buffalo. This might indicate CHS buffalo protect RBCs from heat injury. Hb is associated with the delivery of oxygen from the lungs to various other tissues. High levels of serum Hb protect the red blood cells from oxidative stress [46]. Hb increases may be due to low oxygen pressure and saturation, or to an improved resistance to ROS [13]. In contrast, cooling increased blood Hb concentrations in CHS Murrah buffalo [47]. High Hb levels may alleviate the deleterious effect of CHS and hypoxia. However, one study showed that HS decreased blood Hb concentration as compared to normal temperatures [48], which may be because the acute HS animals in that study were exposed to extremely high temperatures (40 ± 2°C).

Our CHS buffalo had higher serum Hb as compared to TN buffalo. CHS buffalo also had significantly higher concentrations of HBA1 than the TN buffalo, indicating that high HBA1 concentrations may alleviate the tissue and organ hypoxia caused by high respiratory rates. It has been shown that HBA1 plays an important role in increasing blood flow to peripheral tissues. CHS buffalo also had significantly

lower levels of MCHC and MCH, as well as significantly higher levels of HCT and MCV. This might indicate that CHS dairy buffalo maintain a normal oxygen supply by modulating crucial blood parameters.

HS animals decrease nutrient intake, leading to a negative energy balance. Because fatty acid oxidation produces more heat (146 ATP) than does carbohydrate (38 ATP), heat-stressed animals decrease fatty acid oxidation [49]. LPL is synthesized at the surface of the vascular endothelium and released into the blood. LPL hydrolyzes circulating triacylglycerides to free fatty acids, promoting fat synthesis while decreasing the production of ATP and heat [50]. In addition to decreasing heat production, fat deposition is beneficial under HS as fat insulates the body to decrease solar radiant heat absorption [14]. Indeed, low levels of glycerol in the plasma of ruminants were found in summer [51]. However, few studies have focused on serum profiles of LPL abundance. LPL levels in pig adipose tissue increased in response to mild HS [52], as did adipogenesis in porcine adipocyte [53]. LPL activity increased in the plasma and muscle of HS rats, but not in the white adipose tissue [54]. We found that serum LPL abundance decreased in response to CHS. We thus speculated that dairy buffalo, unlike monogastric animals, adapt to CHS by decreasing fatty acid oxidation to reduce heat production.

Conclusion

Results of the present experiment indicated that, in dairy buffalo, pathways associated with oxidation-reduction, hydrolysis, protein-mis-folding repair, and oxygen delivery were activated by CHS, and that LPL, GPX3, LL–37, CP, and HBA1 played cooperative roles to mitigate the effects of CHS. Dairy buffaloes adapt to chronic heat stress and hypoxia with high levels of RBCs, HBA1 and CP increased blood oxygen delivery capacity.

Abbreviations

CATHL2 (LL–37), cathelicidin–2; CP, ceruloplasmin; GPX3, glutathione peroxidase 3; Hb, hemoglobin; HBA1, hemoglobin subunit alpha 1; HCT, hematocrit; HS, heat stress; LFQ, label-free quantification; LPL, Lipase; MCHC, mean corpuscular hemoglobin concentration; MCH, mean corpuscular hemoglobin; MCV, mean corpuscular volume; PLT, platelet hematocrit; PRM, parallel reaction monitoring; RBC, red blood cell count; ROS, reactive oxygen species; RR, Respiration rates; SRM/MRM, Single or multiple reaction monitoring; THI, Temperature-humidity index; WBC, white blood cell count; TN, thermal-neutral conditions

Declarations

Funding

This work was supported by grants Yunnan Agricultural Foundation Projects of China (2017FG001–008) and China National Science Foundation (31560626).

Acknowledgements

We thank the staff of Shanghai Applied Protein Technology Co. Ltd for their technical assistance.

Authors' contributions

Ping Liu contributed to performance of the study. Lulu Guo contributed to the data analysis. Huaming Mao supervised the project. Zhaobing Gu designed the study and write the manuscript. All authors submitted comments on drafts, and read and approved the final manuscript.

Availability of data and materials

All data generated or analyzed during this study are included in this published article or supplementary information.

Ethics approval and consent to participate

Animals were treated according to the strictures of the Animal Welfare Act, as issued by Animal Ethics Committee of Yunnan Province, China in 2007.

Consent for publication

Not applicable.

Competing interests

The authors declare that they have no competing interests.

References

1. Baumgard LH, Rhoads RP. Effects of heat stress on postabsorptive metabolism and energetics. Annu Rev Anim Biosci. 2013; 1(1): 311–337.

2. Chanda T, Debnath GK, Khan KI, Rahman MM, Chanda GC. Impact of heat stress on milk yield and composition in early lactation of Holstein Friesian crossbred cattle. Bang J Anim Sci. 2017; 46(3): 192–197.

3. Ganaie AH, Shanker G, Bumla NA, Ghasura RS, Mir NA, Wani SA, Dudhatra GB. Biochemical and physiological changes during thermal stress in bovines: a review. J Vet Sci Technol. 2013; 4(1): 423–430.

4. Kapila N, Kishore A, Sodhi M, Sodhi M, Sharma A, Mohanty AK, Kumar P, Mukesh M. Temporal changes in mRNA expression of heat shock protein genes in mammary epithelial cells of riverine buffalo in

response to heat stress in vitro. International Journal of Animal Biotechnology. 2013; 2013(3): 5–9.
5. Dunshea FR, Leury BJ, Fahri F, Digiacomo K, Hung A, Chauhan S, Clarke I J, Collier R, Little S, Baumgard L, Gaughan JB. Amelioration of thermal stress impacts in dairy cows. Anim Prod Sci. 2013; 53(9): 965–975.
6. Ghosh CP, Kesh SS, Tudu NK, Datta S. Heat Stress in Dairy Animals - Its Impact and Remedies: a Review. Int J App Pure Biosci. 2017; 5:953–965.
7. Slimen B, Najar T, Ghram A, Abdrrabba M. Heat stress effects on livestock: molecular, cellular and metabolic aspects, a review. J Anim Physiol An A. 2016; 100(3): 401–412.
8. Bassols A, Turk R, Roncada P. A proteomics perspective: from animal welfare to food safety. Curr Protein Pept Sci. 2014; 15(2): 156–168.
9. Peterson AC, Russell JD, Bailey DJ, Westphall MS. Parallel reaction monitoring for high resolution and high mass accuracy quantitative, targeted proteomics. Mol Cell Proteomics. 2012; 11(11): 1475–1488.
10. Sweredoski MJ, Moradian A, Raedle M, Franco C, Hess S. High resolution parallel reaction monitoring with electron transfer dissociation for middle-down proteomics. Anal Chem. 2015; 87(16): 8360–8366.
11. Liu L, Wang A, Chen J. Blood-based amyloid and tau biomarker tests for alzheimerâs disease. Neuroscience & Biomedical Engineering. 2016; 4(1): 4–13.
12. Lee S, Bao J, Zhou G, Shapiro J, Xu J, Shi RZ, Lu X, Clark T, Johnson D, Kim YC, Wing C, Tseng C, Sun M, Lin W, Wang J, Yang H, Wang J, Du W, Wu CI, Zhang X, Wang SM. Detecting novel low-abundant transcripts in Drosophila. RNA. 2005; 11(6):939–946.
13. Tucker CB, Rogers AR, Schütz KE. Effect of solar radiation on dairy cattle behaviour: use of shade and body temperature in a pasture-based system. Appl Anim Behav Sci. 2008; 109(2–4): 141–154
14. Wisniewski JR,Zougman A, Nagaraj N, Mann M. Universal sample preparation method for proteome analysis. Nat Methods. 2009; 6(5): 359–362.
15. Cox J, Mann M. MaxQuant enables high peptide identification rates, individualized p.p.b.-range mass accuracies and proteome-wide protein quantification. Nat Biotechnol. 2008; 26(12): 1367–1372.
16. MacLean B, Tomazela DM, Shulman N, Chambers M, Finney GL, Frewen B, Kern R, Tabb DL, Liebler DC, MacCoss MJ. Skyline: an open source document editor for creating and analyzing targeted proteomics experiments. Bioinformatics. 2010; 26(7): 966–968.
17. Sturm R, Sheynkman G, Booth C, Smith LM, Pedersen JA, Li L. Absolute quantification of prion protein 90–231 using stable isotope-labeled chymotryptic peptide standards in a LC-MRM AQUA workflow. J Am Soc Mass Spectrom. 2012; 23: 1522–1533.
18. Lin MM, Fang JB, Qi XJ, Li YK, Chen JY, Sun LM, Zhong YP. iTRAQ-based quantitative proteomic analysis reveals alterations in the metabolism of actinidia arguta. Sci Rep. 2017; 7.
19. Gu Z, Li L, Tang S, Li C, Fu X, Shi Z, Mao H. Metabolomics reveals that crossbred dairy buffaloes are more thermotolerant than holstein cows under chronic heat stress. J. Agric. Food Chem. 2018, 66, 12889–12897.
20. Pisoschi A M, Pop A. The role of antioxidants in the chemistry of oxidative stress: a review. Eur J Med Chem. 2015; 97(31): 55–74.
21. Kho CW, Lee PY, Bae KH, Kang S, Cho S, Lee DH, Sun CH, Yi GS, Park BC, Park SG. Gpx3-dependent responses against oxidative stress in Saccharomyces cerevisiae. J Microbiol Biotechnol. 2008; 18: 270–

282.
22. Pan L, Bu DP, Wang JQ, Cheng J B, Sun XZ, Zhou LY, Qin JJ, Zhang XK, Yuan YM. Effects of Radix Bupleuri extract supplementation on lactation performance and rumen fermentation in heat-stressed lactating Holstein cows. Anim Feed Sci Tech. 2014; 187: 1–8.
23. Akbarian A, Golian A, Kermanshahi H, De SS, Michiels J. Antioxidant enzyme activities, plasma hormone levels and serum metabolites of finishing broiler chickens reared under high ambient temperature and fed lemon and orange peel extracts and curcuma xanthorrhiza essential oil. J. Anim Physiol An N. 2015; 99(1): 150–162.
24. Cheng JB, Fan CY, Sun XZ, Wang JQ, Zheng N, Zhang XK, Qin JJ, Wang XM. Effects of bupleurum, extract on blood metabolism, antioxidant status and immune function in heat-stressed dairy cows. J Integr Agr. 2018; 17(3): 657–663.
25. Guo J, Gao S, Quan S, Zhang Y, Bu D, Wang J. Blood amino acids profile responding to heat stress in dairy cows. Asian Austral J Anim Sci. 2018; 31(3): 47–53.
26. Zhang JX, Wang R, Xi J, Shen L, Zhu AY, Qi Q, Wang QY, Zhang LJ, Wang FC, Lü HZ, Hu JG. Morroniside protects SK-N-SH human neuroblastoma cells against H_2O_2-induced damage. Int J Mol Med. 2017; 39(3): 603–612.
27. Zhang FJ, Weng XG, Wang JF, Zhou D, Zhang W, Zhai CC, Hou YX, Zhu YH. Effects of temperature-humidity index and chromium supplementation on antioxidant capacity, heat shock protin 72, and cytokine responses of lactating cows. J Anim Sci. 2014; 92(7): 3026–3034.
28. Tomasinsig L, De Conti G, Skerlavaj B, Piccinini R, Mazzilli M, D'Este F, Tossi A, Zanetti M. Broad-spectrum activity against bacterial mastitis pathogens and activation of mammary epithelial cells support a protective role of neutrophil cathelicidins in bovine mastitis. Infect Immun. 2010; 78(4): 1781–1788.
29. Kozłowska E, Wysokiński A, Brzezińska-Błaszczyk E. Serum levels of peptide cathelicidin ll–37 in elderly patients with depression. Psychiat Res. 2017; 255: 156–160.
30. Radek KA, Elias PM, Taupenot L, Mahata SK, O'Connor DT, Gallo RL. Neuroendocrine nicotinic receptor activation increases susceptibility to bacterial infections by suppressing antimicrobial peptide production. Cell Host Microbe. 2010; 8(6): 277–289.
31. Young-Speirs M, Drouin D, Cavalcante PA, Barkema HW, Cobo ER. Host defense cathelicidins in cattle: types, production, bioactive functions and potential therapeutic and diagnostic applications. Int J Antimicrob Ag. 2018; 51(6): 813–821.
32. McNamara TC, Keen JT, Simmons GH, Alexander LM, Wong BJ. Endothelial nitric oxide synthase mediates the nitric oxide component of reflex cutaneous vasodilatation during dynamic exercise in humans. J Physiol. 2014; 592(3): 5317–5326.
33. Main PA, Angley MT, O'Doherty C E, Thomas P, Fenech M. The potential role of the antioxidant and detoxification properties of glutathione in autism spectrum disorders: a systematic review and meta-analysis. Nutr Metab. 2012; 9(1): 35.
34. Xu X, Leng JY, Gao F, Zhao ZA, Deng WB, Liang XH, Zhang YJ, Zhang ZR, Li M, Sha AG, Yang ZM. Differential expression and anti-oxidant function of glutathione peroxidase 3 in mouse uterus during decidualization. FEBS Letters. 2014; 588(9): 1580–1589.

35. Aggarwal A, Upadhyay RC. Studies on evaporative heat loss from skin and pulmonary surfaces in male buffaloes exposed to solar radiations. Buffalo J. 1998; 14(2): 179–187.
36. GonzálezAlonso J, Calbet JA. Reductions in systemic and skeletal muscle blood flow and oxygen delivery limit maximal aerobic capacity in humans. Circulation. 2003; 107(6): 824–830.
37. Pizzuti C, Rombo SE. Algorithms and tools for protein–protein interaction networks clustering, with a special focus on population-based stochastic methods. Bioinformatics. 2014; 30(10):1343–1352.
38. Sheeba V, Arunachalam P, Swarnalatha K. Correlation of hemoglobin with creatinine clearance, antioxidant status, lipid peroxidation and ceruloplasmin in patients with chronic kidney disease. Inter J Res Med Sci. 2016; 4: 4487–4492.
39. Tetik VA, Harman E, Bozok ÇV, Kayıkçıoğlu M, Vardarl E, Zengi A, Şahin AK, Eroğlu Z. Polymorphisms of lipid metabolism enzyme-coding genes in patients with diabetic dyslipidemia. Anatol J Cardiol. 2017; 17(4): 313–321.
40. Collin A, Lebreton Y, Fillaut M, Vincent A, Thomas F, Herpin P. Effects of exposure to high temperature and feeding level on regional blood flow and oxidative capacity of tissues in piglets. Exp Physiol. 2010; 86(1): 83–91.
41. Ogoh S, Sato K, Okazaki K, Miyamoto T, Hirasawa A, Morimoto K, Shibasaki M. Blood flow distribution during heat stress: cerebral and systemic blood flow. J Cerebr Blood F Met. 2013; 33(12):1915–1920.
42. Pearce SC, Mani V, Boddicker L, Johnson JS, Weber TE, Ross JW, Rhoads RP, Baumgard LH, Gabler NK. Heat stress reduces intestinal barrier integrity and favors intestinal glucose transport in growing pigs. Plos One. 2013; 8(8): e70215
43. Liu Z, Sun X, Tang J, Tang Y, Tong H, Wen Q, Liu Y, Su L. Intestinal inflammation and tissue injury in response to heat stress and cooling treatment in mice. Mol Med Rep. 2011; 4(3): 437–443.
44. Takahashi M. Heat stress on reproductive function and fertility in mammals. Reprod Med Biol. 2012; 11(1): 37–47.
45. Habeeb AAM. The role of insulin in improving productivity of heat stressed farm animals with different techniques. Zagazig, Egypt: Ph.D. Thesis, Faculty of Agriculture, Zagazig University, Zagazig, 1987.
46. Mohanty JG, Nagababu E, Rifkind JM. Red blood cell oxidative stress impairs oxygen delivery and induces red blood cell aging. Front Physiol. 2014; 5: 84.
47. Brijesh Y, Vijay P, Sarvajeet Y, Yajuvendra S, Vinod K, Rajneesh S. Effect of misting and wallowing cooling systems on milk yield, blood and physiological variables during heat stress in lactating Murrah buffalo. J Anim Sci Technol. 2016; 58(1): 2.
48. Sivakumar AVN, Singh G, Varshney VP. Antioxidants supplementation on acid base balance during heat stress in goats. Asian Austral J Anim Sci. 2010; 23(11): 1462–1468.
49. Xin WU, Li ZY, Jia AF, Su HG, Hu CH, Zhang MH, Feng JH. Effects of high ambient temperature on lipid metabolism in finishing pigs. J Integr Agr. 2016; 15(2): 391–396.
50. Ricartjané D, Cejudomartín P, Peinadoonsurbe J, Lópeztejero MD, Llobera M. Changes in lipoprotein lipase modulate tissue energy supply during stress. J Appl Physiol. 2005; 99(4): 1343–1351.
51. Larsen TS, Lagercrantz H, Riemersma RA, Blix AS. Seasonal changes in blood lipids, adrenaline, noradrenaline, glucose and insulin in norwegian reindeer. Acta Physiol. 2010; 124(1): 53–59.

52. Kouba M, Hermier D, Dividich JL. Influence of a high ambient temperature on lipid metabolism in the growing pig. J Anim Sci. 2001; 79(1): 81–87.
53. Qu H, Donkin SS, Ajuwon KM. Heat stress enhances adipogenic differentiation of subcutaneous fat depot-derived porcine stromovascular cells. J Anim Sci. 2015; 93(8): 3832–3842.
54. Mayer ML, Hancock RE. Cathelicidins link the endocrine and immune systems. Cell Host Microbe. 2010; 7(4): 257–259.

Tables

Table 1 Low-abundant differentially expressed serum proteins in CHS buffalo as compared to TN buffalo, as indicated by label-free quantitation

Protein ID	Protein symbol	Protein name	Fold change	P
Q9TSN7	HBA1	Hemoglobin subunit alpha1	3.76	0.036
L8I5R0	CP	Ceruloplasmin [EC:1.16.3.1]	1.50	0.024
A0A0A7V3V9	CAMP (LL-37)	Cathelicidin-2, CATHL2	1.84	0.026
D2U6Z5	CP	Ceruloplasmin [EC:1.16.3.1]	1.58	0.035
P63103	YWHAZ	YWHAZ	0.35	0.001
P37141	GPX3	Glutathione peroxidase 3 [EC:1.11.1.9]	0.35	0.006
K9MNT8	RETN	Resistin	0.47	0.022
Q2KII3	HAVCR1	Hepatitis A virus cellular receptor 1 N-terminal domain containing protein	0.44	0.030
P62261	YWHAE	Protein epsilon	0.52	0.001
G5E5V0	CPN1	Carboxypeptidase N catalytic chain precursor	0.63	0.007
E1ACW2	LPL	Lipoprotein lipase [EC:3.1.1.34]	0.59	0.010
A7Z057	YWHAG	Protein gamma	0.51	0.017
L8I9P7	CD14	Monocyte differentiation antigen	0.65	0.020
L8I6N0	CHST4	Glycosylation-dependent cell adhesion molecule 1	0.59	0.022
L8IDW3	THBS4	Thrombospondin-4	0.57	0.033
L8IZ21	SERPINF1	Pigment epithelium-derived factor	0.65	0.034
L8HYL8	PLA1A	Phospholipase A1 member A [EC:3.1.1.-]	0.56	0.045

Table 2 Molecular function of 17 low-abundant differentially expressed serum proteins in CHS buffalo as compared to TN buffalo (protein details are given in Table 1)

GO_ID	Molecular Function	Protein ID
GO:0003824	Catalytic activity	L8I5R0, P63103, P62261, A7Z057, E1ACW2, P37141, G5E5V0, D2U6Z5, L8HYL8
GO:0016491	Oxidoreductase activity	L8I5R0, P63103, P62261, A7Z057, P37141, D2U6Z5
GO:0016209	Antioxidant activity	P37141
GO:0016787	Hydrolase activity	E1ACW2, G5E5V0, L8HYL8
GO:0005215	Transporter activity	Q9TSN7
GO:0019825	Oxygen binding	Q9TSN7
GO:0043167	Ion binding	L8I5R0, Q9TSN7, L8IDW3, P62261, E1ACW2, D2U6Z5, G5E5V0, L8I6N0
GO:0031625	Ubiquitin protein ligase binding	P63103, P62261

Table 3 Biological process of 17 low-abundant differentially expressed serum proteins in CHS buffalo as compared to TN buffalo (protein details are given in Table 1)

GO_ID	Biological process	Protein ID
GO:0006950	Response to stress	P63103, L8IDW3, L8I9P7, P62261, P37141, P80012, A0A0A7V3V9
GO:0055114	Oxidation-reduction process	L8I5R0, P63103, P62261, A7Z057, P37141, D2U6Z5
GO:0009056	Catabolic process	K9MNT8, E1ACW2, L8HYL8
GO:0050790	Regulation of catalytic activity	P62261, A7Z057, L8IZ21
GO:0042592	Homeostatic process	L8I5R0, E1ACW2, D2U6Z5
GO:0006629	Lipid metabolic process	K9MNT8, E1ACW2, L8HYL8
GO:0006810	Metal ion and gas transportation and homeostasis	L8I5R0, P63103, Q9TSN7, L8I9P7, P62261, A7Z057, D2U6Z5
GO:1903522	Regulation of blood circulation	P62261

Figures

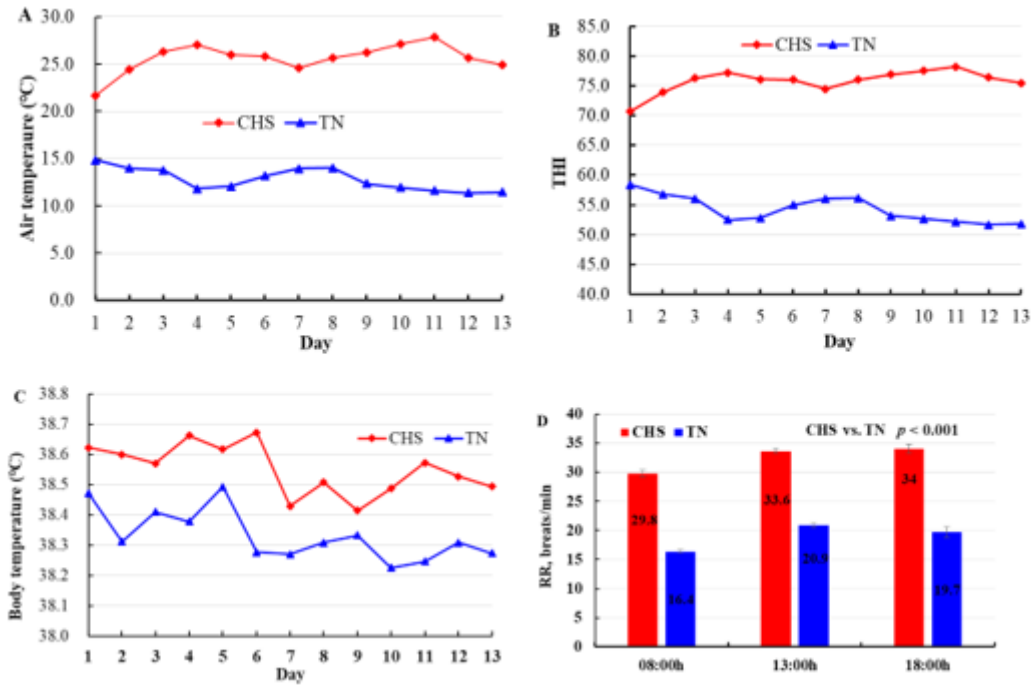

Figure 1

Temperature, THI, respiratory rates (RR) and body temperature for CHS (red mark) and TN (blue mark) buffaloes. (a) air temperature, (b) THI (temperature humidity indexes), (c) body temperature and (d) respiratory rates.

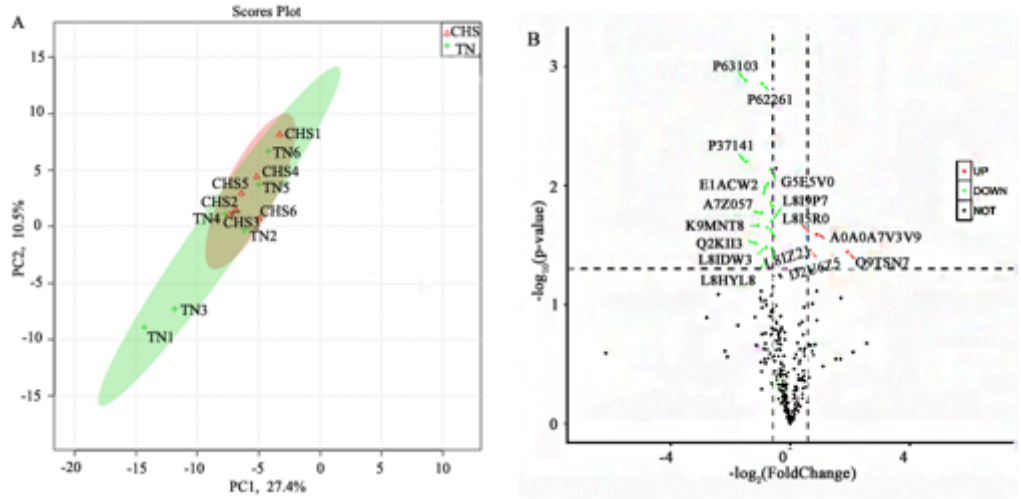

Figure 2

Quantitative proteomic comparison of serum samples of heat-stressed and normal-temperature buffalo. (a) Principal components analysis (PCA). (b) Volcano plot representation of moderated t-test analysis. Each point represents one protein. Fold change calculated based on the average of six samples. The horizontal bar represents a q-value cutoff of 0.01. Significantly more abundant proteins in the heat-stress

buffalo are shown in red; significantly less abundant proteins are shown in green. The significantly more abundant proteins were verified with parallel reaction monitoring analysis.

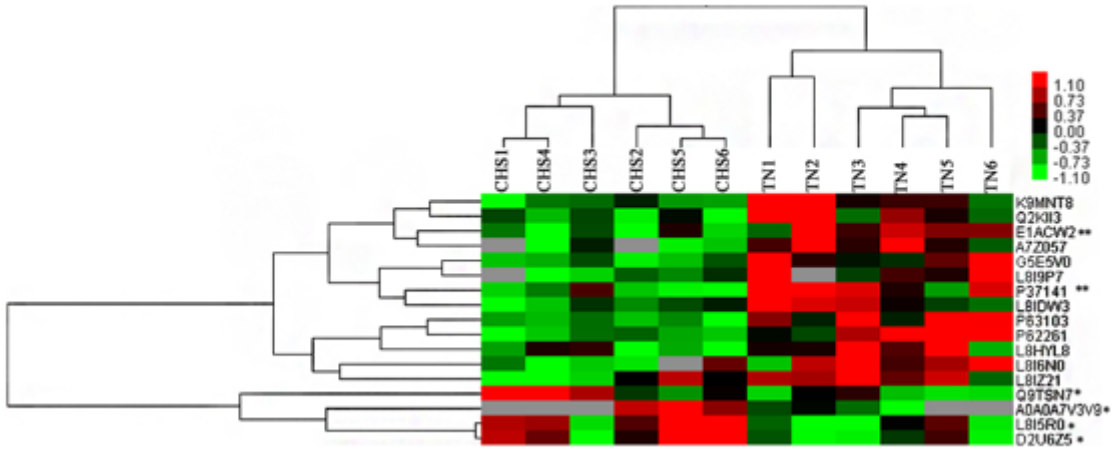

Figure 3

Hierarchical clustering of the proteins identified as differentially abundant in the heat-stressed buffalo as compared to the normal-temperature buffalo with label-free quantification analysis. Proteins are in rows; protein details are given in Table 1. Colors indicate level of abundance. CHS1–6: Chronic heat stress buffalo 1–6; TN1–6: Thermoneutral buffalo 1–6. Asterisks indicate proteins that are significantly differently abundant between groups: *p < 0.05, **p < 0.01.

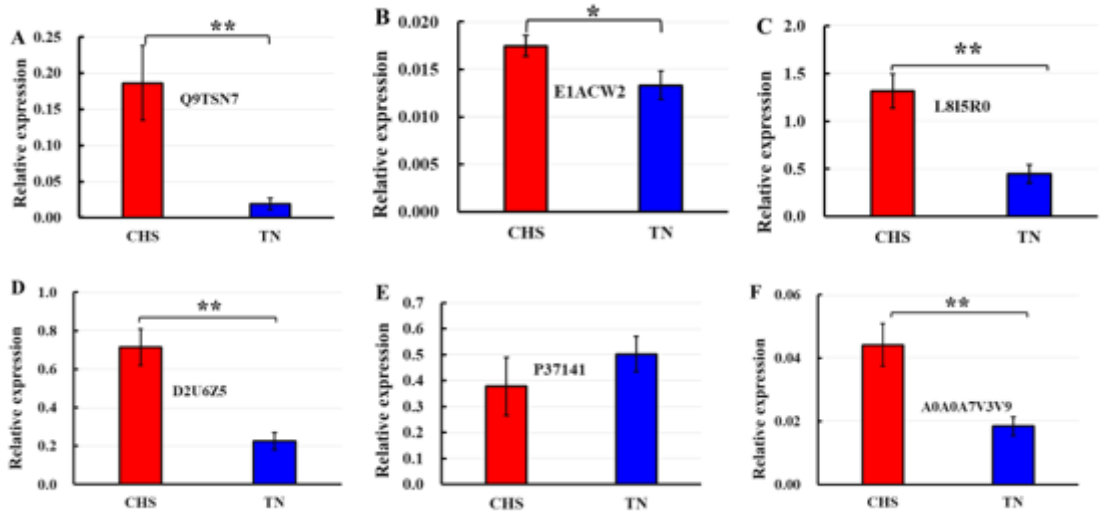

Figure 4

Parallel reaction monitoring verification of five of the proteins indicated to be significantly differentially abundant by label-free quantification. CHS: Chronic heat stress buffalo (red bars); TN: thermoneutral buffalo (blue bars). Bars represent means (n = 6) ± standard error. Asterisks indicate significant

differences in abundance between the two groups: *p < 0.05, **p < 0.01. L8I5R0 and D2U6Z5 represent CP. For full protein names, please refer to Table 1.

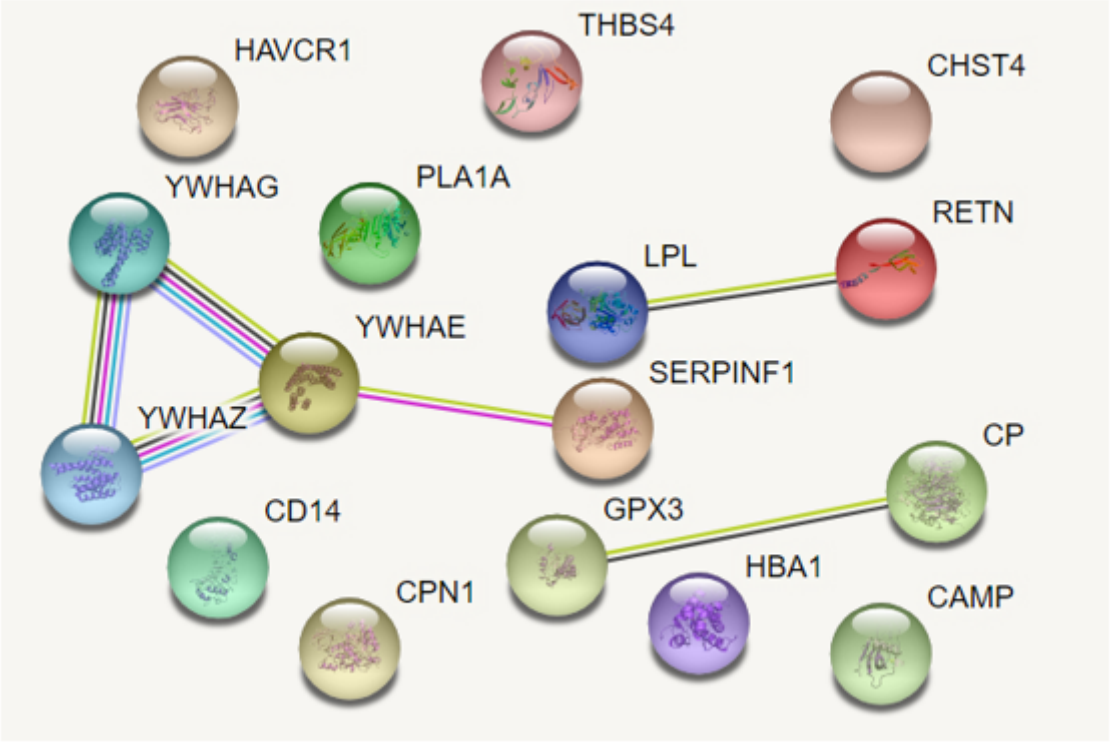

Figure 5

Protein–protein interaction network including the proteins differentially abundant in chronic heat stress buffalo as compared to thermoneutral buffalo. Blue edges indicate co-occurrence evidence; purple edges indicate experimental evidence; yellow edges indicate text-mining evidence; light blue edges indicate database evidence; and black edges indicate co-expression evidence. For full protein names, please refer to Table 1.

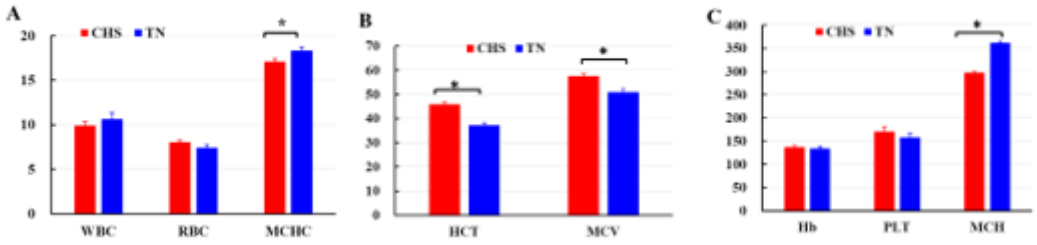

Figure 6

Blood parameters of chronic heat stress (CHS, red bars) and thermoneutral buffalo (TN, blue bars) buffalo. WBC: white blood cells (×109); RBC: red blood cells (×1012); MCHC: mean corpuscular hemoglobin concentration (g/L); MCV: mean corpuscular volume (fL); Hb: hemoglobin (g/L); MCH: mean corpuscular volume (pg); PLT: platelet hematocrit (×109). Bars represent means (n = 6) ± standard error. Asterisks indicate significant differences in abundance between the two groups: *p < 0.05.

Supplementary Files

This is a list of supplementary files associated with this preprint. Click to download.

- supplement1.pdf
- supplement2.xlsx
- supplement3.xlsx
- supplement4.xlsx
- supplement5.pdf
- supplement6.xlsx